Growth Kinetics of Boride Layers on Iron-Chromium Alloys and their Dry Abrasive Wear Resistance

V.I. Dybkov, L.V. Goncharuk, V.G. Khoruzha, K.A. Meleshevich, A.V. Samelyuk,
V.R. Sidorko**,** Institute for Problems of Materials Science, Department of Physical Chemistry of Inorganic Materials, Kyiv 03180, Ukraine

Keywords: Fe–Cr alloys, 13% Cr Steel, Amorphous Boron, Boride layers, Growth kinetics

Abstract

Two boride layers based on the FeB and Fe_2B compounds are formed at the interface between Fe–Cr alloys (10 and 25% Cr) or a 13% Cr steel and boron at 850-950 °C and reaction times up to 12 h. With a Fe–10% Cr alloy and the steel, these are (Fe,Cr)B and $(Fe,Cr)_2B$, the average chromium content being around 8 at.% in the former and 9 at.% in the latter. In the case of a Fe–25% Cr alloy, the outer boride layer comprises the (Fe,Cr)B and (Cr,Fe)B phases. Similarly, the inner boride layer consists of the $(Fe,Cr)_2B$ and $(Cr,Fe)_2B$ phases. The characteristic feature of both boride layers on the surface of these materials is a pronounced texture. The strongest reflections are {002} and {020} for the orthorhombic FeB phase and {002} for the tetragonal Fe_2B phase. The diffusional layer-growth kinetics are described by a system of two non-linear differential equations. With a Fe–10% Cr alloy, a Fe–25% Cr alloy and the steel, respective microhardness values are 13.0, 21.0 and 17.9 GPa for the outer boride layer, 11.8, 18.0 and 16.1 GPa for the inner layer, and 1.3, 1.35 and 5.9 GPa for the base material. The ratio of dry wear resistance values, found from mass loss measurements, of the outer FeB layer for a Fe-10% Cr alloy, the steel and a Fe-25% Cr alloy is 1:1.2:30. Even though the chromium content of a Fe-25% Cr alloy is only 2.5 times greater than that of a Fe-10% Cr alloy, the wear resistance of the former is more than an order of magnitude greater than that of the latter.

Introduction

Boriding is one of widespread thermochemical surface treatments used to improve service characteristics (hardness, mechanical and corrosive wear resistance, etc.) of metals, alloys and steels [1-3]. Iron borides Fe_2B and FeB are known to exist in the Fe–B binary system [4-7]. With iron, its alloys and steels, one-phase or two-phase coatings can therefore be obtained, depending on boriding techniques employed and temperature-time conditions of a boriding procedure.

The properties of boride coatings are to a large extent dependent on the amount of alloying elements and impurities present in a base material. In the case of materials of complicated chemical composition, for example steels, it is not so easy to separate the effect of a particular element from that of others. Therefore, experiments with binary alloys are desirable. In this work, the data on the interaction of Fe–Cr alloys (10 and 25 % Cr) and a commercial 13% Cr steel with boron in a mixture of amorphous boron powder and 5% KBF_4 at 850-950 °C are presented, with the main emphasis on establishing the boride layer-growth kinetics that received comparatively little attention. Also, the results of dry abrasive wear resistance tests of boride coatings formed on the surface of those materials are reported.

Experimental Procedure

Materials and specimens

The materials used included high-purity iron powder (99.98% Fe), electrolytic-grade chromium platelets (99.98% Cr), a commercial 13% Cr steel rod in the as-received condition (without any additional heat treatment), amorphous boron and analytical-grade KBF_4. The content of main components of the steel was 85.2% Fe, 13.6% Cr, 0.38% C, 0.30% Mn, 0.30% Si and 0.20% Ni. All contents are given in mass percent if otherwise not stated. The steel microstructure consisted of the body centered cubic α-phase (ferrite) with fine inclusions of carbides $Me_{23}C_6$ (Me = Cr, Fe).

Initially, the boron powder contained 98.3% B, 0.04% C, 1.6% O and insignificant amounts of Si, Cu, Mg (< 0.01% each) and Fe (< 0.001%). Before the boriding experiments, the powder was first heated slowly in vacuum up to 1450 ^{o}C and then calcined at this temperature for 2 h in an atmosphere of argon at a pressure of 2.5×10^4 Pa to remove volatile oxides. KBF_4 was preliminary dried in steps at 95, 110, 130 and 170 ^{o}C (24 h at each temperature).

Cylindrical rods of Fe-Cr alloys were prepared by arc-melting of appropriate metals under argon, with subsequent casting of the melts into water-cooled copper crucibles. The rods were annealed to ensure their homogenization at a temperature of 1100 ^{o}C for 2h in an argon atmosphere at a pressure of 2.5×10^4 Pa.

Specimens in the form of tablets, 11.28 mm in diameter and 5.5 mm high, were machined from the Fe-Cr alloy or steel rods. Flat sides (1 cm^2 area) of the tablets were ground and polished mechanically.

Experimental methods

The vacuum device VPBD-2S employed for boriding Fe-Cr alloy and steel samples has been described elsewhere [8]. The experiment was carried out in an alumina crucible, 13 mm inner diameter and 40 mm high.

A Fe-Cr alloy or steel tablet was embedded into a mixture of boron powder with 5% KBF_4 as an activator. This amount of KBF_4 appears to be optimum [1, 9]. The mixture was then slightly pressed, and a load of 8.5 g (a low-carbon steel cylinder) was placed on top. The crucible was closed with a low-carbon steel lid and placed into a steel-sheet holder, mounted to a guide rod capable of moving in the vertical direction.

The chamber was pumped to a pressure of about 10 Pa and filled with high-purity argon (99.999 vol.% Ar). This procedure was repeated twice. Then, the chamber was again pumped and filled with argon at a pressure of 2.5×10^4 Pa, and heating was started. During heating, the crucible with its contents was in the cold zone above the furnace. After the required temperature in the range of 850-950 ^{o}C had been reached in the furnace, the crucible, pre-heated to about 400 ^{o}C, was moved into its middle part. After an initial drop, the temperature attained its pre-determined value in 4-5 min and was then maintained constant within ± 1^{o}C with the help of an automatic thermoregulator VRT-3. The temperature measurements were carried out using a Pt-PtRh thermocouple. The experiments were carried out at temperatures of 850, 900 and 950 ^{o}C. Their duration was 3600-43200 s (1-12 h).

After the experiment, the tablet coated with boride layers was cut along the cylindrical axis into two unequal parts (4 and 7 mm) using an electric-spark machine. Its greater part was embedded into a cold-setting epoxy resin and used to prepare a metallographic cross-section. The lesser part was used for X-ray diffraction investigations (plain-view samples).

Characterization of initial materials and boride layers was carried out with the help of metallography, X-ray and chemical analyses, and electron probe microanalysis (EPMA). The thickness of boride layers was measured using an optical microscope MIM-7 equipped with a HP Photosmart 720 camera. The chemical composition of the layers and the concentration profiles of the elements in the transition zone between reacting phases were obtained using electron probe microanalyzers JEOL Superprobe 733 and CAMECA Camebax SX50. The beam spot diameter and the phase volume analyzed at each point were estimated to be about 1 μm and 2 μm^3, respectively.

X-ray diffraction patterns were taken immediately from the surface of tablet samples on a DRON-3 apparatus using Cu K_α radiation. When taking the first pattern, no polishing of a borided sample was applied (section 0). Then, 20-40 μm of a boride layer was removed by grinding and subsequent polishing, and another X-ray diffraction pattern was taken (section I). This procedure was repeated at a step of 20-30 μm until the base material was reached (sections II to V or VI). Six or seven X-ray diffraction patterns were thus taken on each borided sample.

Microhardness measurements on metallographic cross-sections were carried out using a standard PMT-3 tester with the diamond pyramide (Vickers indenter). The load was 0.98 N (100 g).

Abrasive wear resistance tests were carried out on P180 SiC emery paper tape (main fraction grain size 63 μm, maximum 90 μm) using an AWRD-5 device. The velocity of continuous movement of the tape (30 m long) was 0.35 m s^{-1}, while the gauge length during each test was 27.0 m. The load was 50 N (5.1 kg). The working area of tablet samples was 1 cm^2. The wear resistance was determined by means of weighing the samples and measuring their height. Layer-by-layer measurements on the same borided sample allowed the wear characteristics of different boride phases as well as the base material to be determined separately.

Results and Discussion

Phase identity and chemical composition of boride layers

Two boride layers were found to form at the interface of Fe-Cr alloys or the steel and boron at 850-950 ^{o}C and reaction times up to 12 h (Fig. 1). Layer-by-layer X-ray analysis (Fig. 2) and a further comparison of our and literature [10] data showed that with a Fe-10% Cr alloy and the steel the outer layer bordering the boriding agent was the FeB phase, while the inner layer adjacent to the steel base was the Fe_2B phase. Both phases dissolve considerable amounts of chromium. Its distribution within the boride layers is rather irregular, due probably to non-equilibrium conditions of layer formation. The average chromium content found by EPMA measurements is 8 at.% in the FeB layer and 9 at.% in the Fe_2B layer, in agreement with literature values [11].

As seen from cross-sectional micrographs in Figs. 1 and 2, both layers consist of columnar crystals oriented preferentially in the direction of diffusion. Their characteristic feature is a pronounced texture. The strongest reflections are {002} ($2\theta = 63.2$ deg and spacing, $d = 0.148$ nm) and, to a lesser extent, {020} ($2\theta = 32.7$ deg and $d = 0.275$ nm) for the orthorhombic FeB phase, and {002} ($2\theta = 42.7$ deg and $d = 0.212$ nm) for the tetragonal Fe_2B phase. Note that with isotropic microcrystalline samples the strongest reflections are {111}, {200} and {210} for FeB and {211} for Fe_2B.

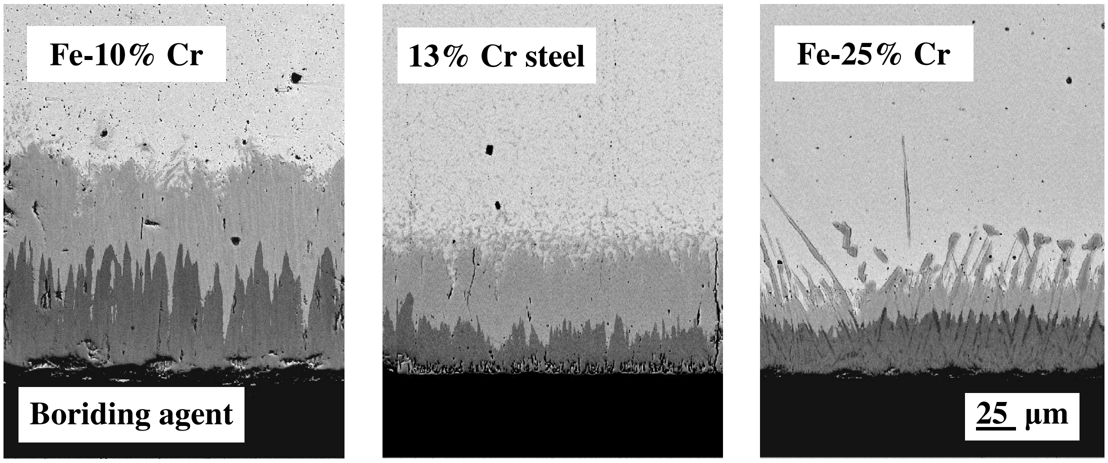

Figure 1 Backscattered electron images of boride layers formed at the interface of Fe-Cr alloys or the steel and boron at a temperature of 950 °C. The darker layer bordering the boriding agent is the FeB phase, while the brighter layer adjacent to the steel base is the Fe_2B phase

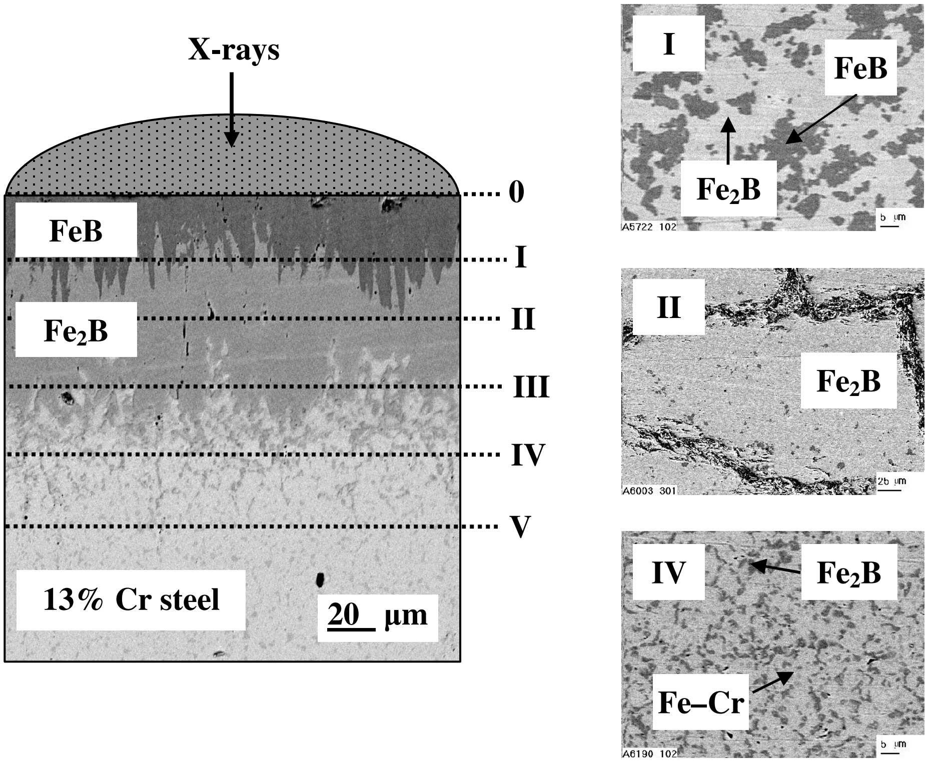

Figure 2 Scheme of X-ray diffraction experiments and microstructures of different sections of the transition zone between 13% Cr steel and boron. Boriding conditions: temperature 950 °C, reaction time 21600 s (6 h)

The larger orientation order is characteristic of the inner portions of both boride layers compared to their near-interface portions, in agreement with findings of other researchers [1, 11, 12]. This is easily explainable because near-interface portions of any boride layer are less equilibrated compared to its inner portions. Therefore, near-interface crystals have less time to align in the preferred direction. The process of formation of the boride-layer texture has been discussed in detail, for example, by Voroshnin and Lyakhovich [1] and recently by Martini et al. [12].

The structure of boride layers on the surface of Fe-25% Cr alloy samples is more complicated. Each of them consists of two phases. As seen from plain-view micrographs of Fig. 3 (right), the outer boride layer consists of distinct brighter and darker regions, with the latter having a peculiar regular arrangement. EPMA measurements indicated that iron prevails in brighter regions, while chromium is dominant in darker regions.

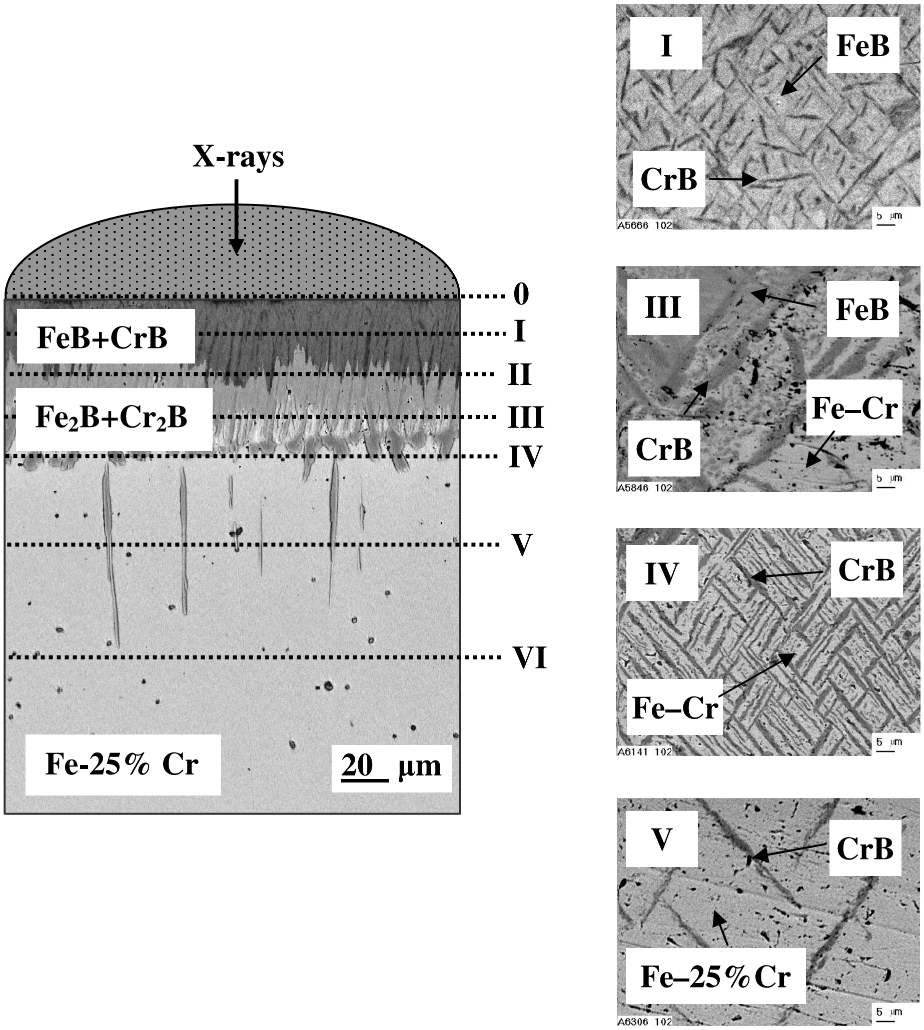

Figure 3 Scheme of X-ray diffraction experiments and microstructures of different sections of the transition zone between a Fe-25% Cr alloy and boron. Boriding conditions: temperature 950 ^{o}C, reaction time 21600 s (6 h)

Hence, compositionally the outer boride layer actually comprises the (Fe,Cr)B and (Cr,Fe)B phases, although X-ray diffraction analysis practically does not show the presence of the CrB phase, probably because, firstly, the FeB and CrB phases have very similar crystal structures [4-6, 10] and, secondly, under non-equilibrium conditions the lattice rearrangement is not completed in view of time limitations. Being far from equilibrium, this layer appears to be single-phase structurally and two-phase compositionally.

The inner boride layer was also found to be non-homogeneous (see the microstructure of section III in Fig. 3). Like the outer layer, it consists of the $(Fe,Cr)_2B$ and $(Cr,Fe)_2B$ phases. Note that the Fe_2B and Cr_2B phases are isomorphous [4-6, 10].

The microstructure of sections IV and V consists of the $(Cr,Fe)_2B$ phase in the decreasing amount and the alloy base somewhat depleted in chromium. Section VI is entirely the alloy base of an initial composition of 25 % Cr.

Layer-growth kinetics

In the presence of BF_3 and other volatile boron-containing compounds that escape from the mixture of amorphous boron and KBF_4 at elevated temperatures, the reaction between initial phases starts simultaneously over the whole interface. With coarse-grained crystalline boron in the absence of any activator, island-like boride layers are usually formed, even at a considerable reaction time [1]. In the present case, continuous layers arose on the solid surface soon (40-60 s) after the start of the boriding procedure. Note that the gas phase only initiates the reaction, while the further growth of boride layers is a solid-state process.

The growth kinetics of compound layers are usually treated using parabolic equations of the type $x^2 = 2k_1t$, where x is the layer thickness, k_1 is the layer growth-rate constant and t is the time [13-15]. For sufficiently thick layers, such equations produce a quite satisfactory fit to the experimental data (Fig. 4).

In fact, however, growth kinetics of the FeB and Fe_2B layers at the diffusional stage of their formation are somewhat more complicated. After compact layers of both borides have formed, their subsequent diffusional growth is due to two partial chemical reactions

$$B_{dif} + Fe_2B = 2FeB \qquad (1_1)$$

$$Fe_{dif} + FeB = Fe_2B \qquad (1_2)$$

taking place at interface 2 (Fig. 5)

Layer-growth kinetics are described by a system of two non-linear equations [16-20]

$$\frac{dx}{dt} = \frac{k_B}{x} - \frac{rg}{p}\frac{k_{Fe}}{y} \qquad (2_1)$$

$$\frac{dy}{dt} = \frac{k_{Fe}}{y} - \frac{q}{sg}\frac{k_B}{x} \qquad (2_2)$$

where x is the FeB layer thickness, y is the Fe_2B layer thickness, k_B is the FeB layer growth-rate constant, k_{Fe} is the Fe_2B layer growth-rate constant, g is the ratio of the molar volumes of the FeB and Fe_2B compounds, $p = q = r = 1$ and $s = 2$ (factors from the chemical formulae of FeB and Fe_2B).

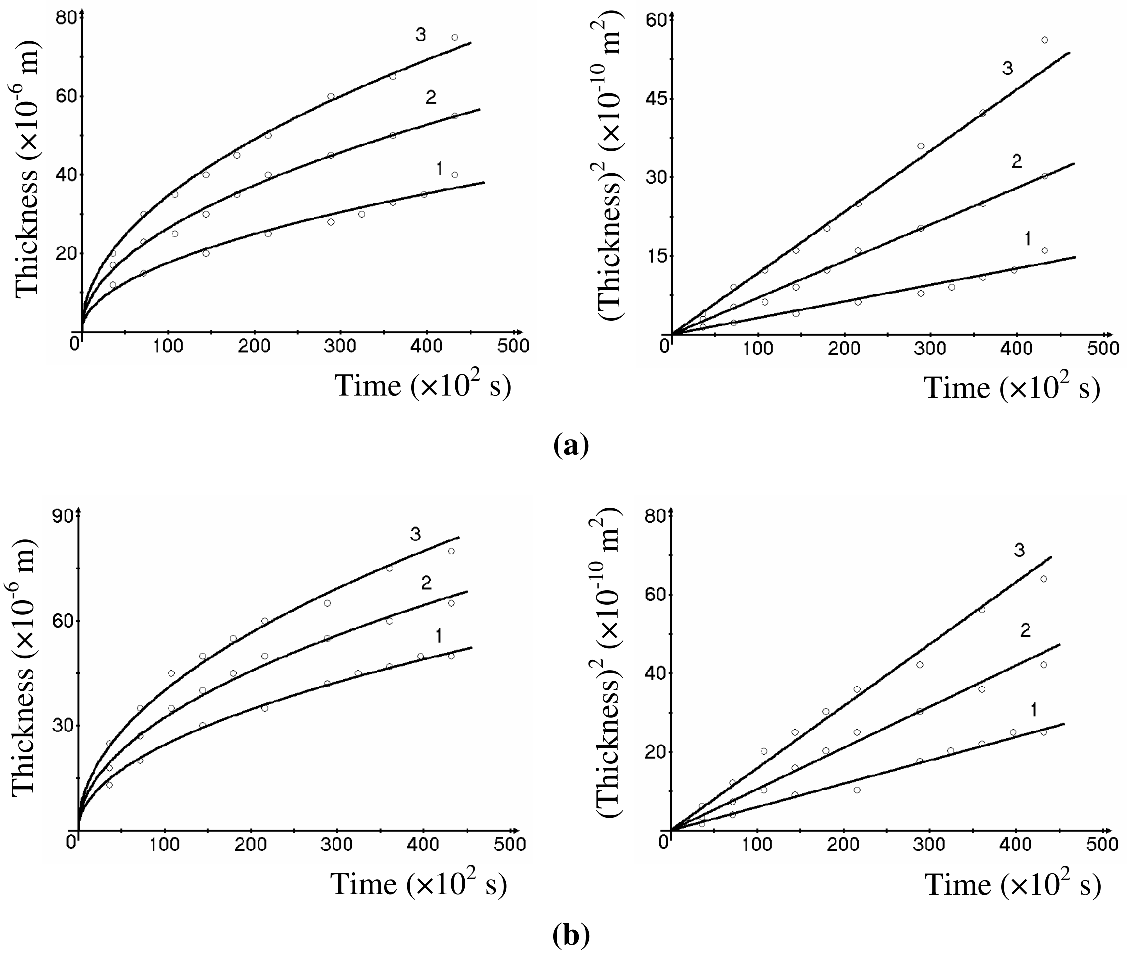

Figure 4 Plots of layer thickness (left) and squared layer thickness (right) versus time for (a) the FeB layer and (b) the Fe_2B layer at a temperature of 850 °C (line 1), 900 °C (line 2) and 950 °C (line 3.

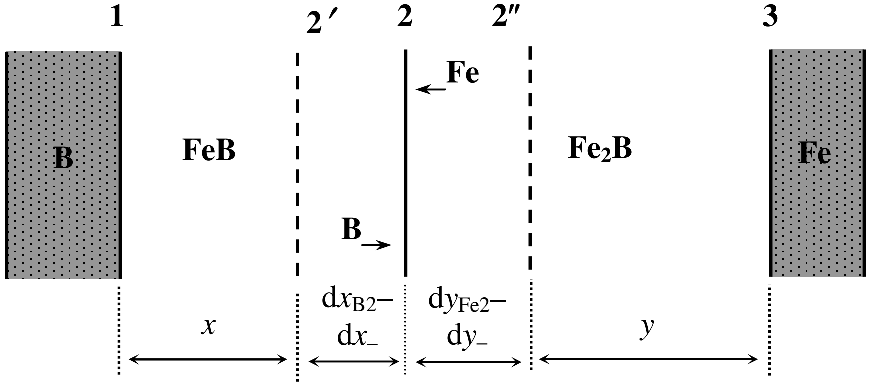

Figure 5 Schematic diagram to illustrate the growth process of two boride layers under conditions of diffusion control. Both layers thicken at their common interface 2. No reactions take place at interfaces 1 and 3 in view of the lack of appropriate diffusing atoms

Even though both boride layers are often considered to grow at the expense of diffusion of the single component boron across their bulks, it is hardly possible with compact layers having no macrodefects and therefore growing by the volume-diffusion mechanism. During diffusional growth, by definition, diffusion across the layer bulks is the rate-determining step, the interface reactions being very fast. It means that all the boron atoms reaching interface 2 react with Fe_2B to form FeB at that interface. Since under conditions of diffusion control the ability of interface 2 to combine those atoms exceeds their diffusional transport across the FeB layer (slow diffusion followed by fast reaction), none of them can diffuse further to interface 3 and react with Fe to form Fe_2B: $B_{dif} + 2Fe = Fe_2B$. This reaction can only take place either under conditions of reaction control when the flux of boron atoms from the initial B-containing phase is sufficient for both boride layers to grow (for more detail, see Ref. [20]) or if the FeB layer is non-protective due to the presence of cracks and other macrodefects. Reaction-controlled growth is only typical of thin compound layers (<1 μm thick). The FeB layer was compact and therefore non-permeable to BF_3 and other gases. Hence, neither of these growth mechanisms could be operative with the materials investigated, except perhaps a Fe-25% Cr alloy.

An obvious criterion of the applicability of Eqs. 2 for treating the diffusional layer-growth kinetics is the constancy of k_B and k_{Fe} over a given range of time, as is the case with boride layers (Table 1). The value of g necessary for calculations of k_B and k_{Fe} was estimated from the densities, $\rho_1 = 6.70 \times 10^3$ kg m^{-3} and $\rho_2 = 7.34 \times 10^3$ kg m^{-3}, of the FeB and Fe_2B compounds [1] and their molecular masses, $M_1 = 66.65$ g mol^{-1} and $M_2 = 122.49$ g mol^{-1}: $g = M_1\rho_2/M_2\rho_1 = 0.60$.

The derivatives were found from the experimental layer thickness-time dependences by the numerical three-point method using a conventional computer program (linear approximation). To find a derivative for a given experimental point, (x_i, t_i), like those on left-hand plots of Fig. 4, data for two neighboring points, (x_{i-1}, t_{i-1}) and (x_{i+1}, t_{i+1}), were also used. Left-hand and right-hand derivatives, $(x_i - x_{i-1})/(t_i - t_{i-1})$ and $(x_{i+1} - x_i)/(t_{i+1} - t_i)$, were first found for this point and a mean value was then calculated. The derivatives could thus be found for all experimental points, excepting clearly end ones, for which a neighboring point is lacking.

As seen in Table 1, the results of calculations of k_B and k_{Fe} by the numerical method are strongly dependent upon a scatter of experimental points. To avoid this, approximation of experimental data with any suitable analytical function is therefore advisable. For example, the use of parabolic relations to approximate the layer thickness-time dependences and then to find the derivatives yields another set of values of k_B and k_{Fe} (Table 2). Since the experimental $x - t$ dependences become smoothed as a result of this procedure (solid lines on left-hand plots of Fig. 4), all values of k_B thus found are identical. The same applies to k_{Fe}. Comparing these with the average values of k_B and k_{Fe} found numerically from the experimental points, it may be concluded that both sets of the constants agree fairly well, providing evidence for the validity of the analytical treatment employed.

The temperature dependence of the layer growth-rate constants is described in the 850-950 °C range by an equation of the Arrhenius type

$$K = K_0 \exp(-E/RT) \qquad (3)$$

where K stands for any layer growth-rate constant, E is the activation energy, R is the gas constant and T is the absolute temperature. Values of K_0 and E are given in Table 3.

Table 1 Thickness and growth constants of boride layers formed at the steel-boron interface at 950 °C

Temperature (°C)	Time ($\times 10^2$ s)	Thickness ($\times 10^{-6}$ m)			k_1 ($\times 10^{-14}$ m^2 s^{-1})			k ($\times 10^{-13}$ m^2 s^{-1})#	
		total	FeB	Fe_2B	total	FeB	Fe_2B	k_B	k_{Fe}
950	36	45	20	25	28.1	5.6	8.7		
	72	65	30	35	29.3	6.3	8.5	4.02	6.60
	108	80	35	45	29.6	5.7	9.3	3.30	6.03
	144	90	40	50	28.1	5.6	8.7	3.17	5.46
	180	100	45	55	27.8	5.6	8.4	3.57	6.00
	216	110	50	60	28.0	5.8	8.3	3.60	5.80
	288	125	60	65	27.1	6.3	7.3	3.57	5.32
	360	140	65	75	27.2	5.9	7.8	1.77	2.98
	432	155	75	80	27.8	6.5	7.4		

Mean values: $k_B = (3.29 \pm 0.83) \times 10^{-13}$ m^2 s^{-1}, $k_{Fe} = (5.45 \pm 0.97) \times 10^{-13}$ m^2 s^{-1}

Table 2 Values of boride layer growth-rate constants found from a parabolic relation, k_1, and from Eqs. 2, k

Alloy	Temperature (°C)	k_1 ($\times 10^{-14}$ m^2 s^{-1})			k ($\times 10^{-13}$ m^2 s^{-1}) from experimental points		k ($\times 10^{-13}$ m^2 s^{-1}) from approximated dependences	
		total	FeB	Fe_2B	k_B	k_{Fe}	k_B	k_{Fe}
10% Cr	850	19.8	4.1	5.9	2.8	4.6	2.5	4.2
	900	30.4	6.6	8.6	4.5	7.1	4.0	6.3
	950	72.4	15.4	21.4	11.0	18.2	9.4	15.4
25% Cr	850	5.3	1.6	1.1	0.92	1.02	0.86	0.96
	900	8.9	3.1	1.7	1.69	1.71	1.60	1.59
	950	16.0	5.0	3.1	2.49	2.69	2.63	2.79
Steel	850	8.8	1.6	3.0	1.21	2.44	1.04	2.01
	900	17.3	3.5	5.3	2.68	4.70	2.17	3.74
	950	28.1	5.9	8.3	3.29	5.45	3.61	5.96

Table 3 Values of K_0 (m^2s^{-1}) and E (kJ mol^{-1}) for Arrhenius-type equations

Alloy	k_1						k_B		k_{Fe}	
	total		FeB		Fe_2B					
	K_0	E	K_0	E	K_0	E	K_0	E	K_0	E
10%Cr	13.22×10^{-7}	147.5	3.89×10^{-7}	150.6	3.46×10^{-7}	146.4	2.16×10^{-6}	149.8	2.79×10^{-6}	147.5
25%Cr	3.74×10^{-8}	125.9	1.86×10^{-8}	130.2	3.27×10^{-9}	118.0	8.07×10^{-8}	128.3	4.32×10^{-8}	121.7
Steel	1.36×10^{-7}	132.8	1.46×10^{-7}	149.4	7.87×10^{-9}	116.4	4.40×10^{-7}	142.2	1.24×10^{-7}	124.3

Microhardness of boride phases

Microhardness is practically constant within both boride layers and slightly diminishes (by 0.1-0.2 GPa) in the base material with increasing distance in the range 0-500 μm from the inner boride layer**.** Its values are presented in Table 4.

Table 4 Microhardness values of boride layers and alloy bases

Material	Fe-10% Cr			13% Cr steel			Fe-25% Cr		
Phase	FeB	Fe_2B	Base	FeB	Fe_2B	Base	FeB	Fe_2B	Base
Microhardness (GPa)	13.0	11.8	1.3	17.9	16.1	5.9	21.0	18.0	1.35

Dry abrasive wear resistance of boride layers

Boriding the alloy or steel tablets for the dry abrasive wear resistance tests was performed at 950°C for 6 h. With Fe-10% Cr alloy and steel samples, similar results were obtained. Three to six consecutive tests on each borided sample, with each test along a fresh track (27.0 m long) on emery paper, were sufficient to reach the base material. In the case of a Fe-10% Cr alloy, the wear resistance of the FeB layer, found from mass loss measurements, is at least ten times greater than that of the alloy base. The Fe_2B layer yields about a fivefold increase in wear resistance of a Fe–10% Cr alloy. With the steel, the wear resistance of the FeB layer is about 25 times greater than that of the steel base. The wear resistance of the Fe_2B layer is around 15 times greater than that of the steel base.

The wear resistance of the outer FeB–CrB layer on the surface of Fe-25% Cr alloy samples proved to be 150 (outermost portions) to 350 (deeper portions) times greater than that of the alloy base. Even though chromium is known to increase the abrasive wear resistance of steels [1, 21], in the present case the extent of its influence appears to be unexpectedly high. Unlike the other materials tested, with this alloy it was impossible to reach the alloy base, carrying out a reasonable amount of consecutive tests. The ratio of wear resistance values of the outer boride layer for a Fe-10% Cr alloy, the steel and a Fe-25% Cr alloy is 1:1.2:30. Even though the chromium content of a Fe-25% Cr alloy is only 2.5 times greater than that of a Fe-10% Cr alloy, the wear resistance of the former is more than an order of magnitude greater than that of the latter. Most probably, the great gain in wear resistance of a Fe–25 % Cr alloy is due to structural (or morphological) rather than compositional reasons.

Conclusions

Two boride layers based on the FeB and Fe_2B compounds are formed at the interface between Fe–Cr alloys (10 and 25% Cr) or a 13% Cr steel and boron at 850-950 ^oC. With a Fe–10% Cr alloy and the steel, these are (Fe,Cr)B and $(Fe,Cr)_2B$, the average chromium content being around 8 at.% in the former and 9 at.% in the latter. In the case of a Fe–25% Cr alloy, the outer layer comprises the (Fe,Cr)B and (Cr,Fe)B phases, whereas the inner layer consists of the $(Fe,Cr)_2B$ and $(Cr,Fe)_2B$ phases.

The characteristic feature of boride layers is a pronounced texture. The strongest reflections are {002} and {020} for the orthorhombic FeB phase and {002} for the tetragonal Fe_2B phase.

Diffusional growth kinetics of the boride layers are close to parabolic. Alternatively, layer-growth kinetics can be described by a system of non-linear differential equations, also producing a good fit to the experimental data.

The ratio of dry wear resistance values of the outer boride layer for a Fe-10% Cr alloy, a commercial 13% Cr steel and a Fe-25% Cr alloy is 1 : 1.2 : 30.

Acknowledgments

This investigation was supported in part by the US Civilian Research and Development Foundation grant No. UKE2-2698-KV-06. The authors thank L.A. Duma for taking X-ray patterns, L.M. Kuzmenko for carrying out chemical analyses, D.M. Pashko for machining nickel specimens and other mechanical work, E.S. Rabotina for making metallic cross-sections, and I.G. Kondratenko and S.V. Bykova for their help in conducting the experiments.

References

[1] L.G. Voroshnin and L.S. Lyakhovich, *Borirovaniye Stali*, Metallurgiya, Moskwa, 1978

[2] H. Kunst, H. Schroll, R. Luetje, K. Wittel, E. Lugscheider, T. Weber, H.R. Eschnauer, and C. Raub, Metals, Surface Treatment, in: *Ullmann's Encyclopedia of Industrial Chemistry*, Vol A16, Verlag Chemie, Weinheim, 1991, p. 427

[3] A.K. Sinha, Boriding (Boronizing), in: A.K. Sinha (Ed.), *Metals Handbook*, ASM International, Metals Park, OH, 1982, p. 844

[4] M. Hansen, *Constitution of binary alloys*, McGraw-Hill, New-York, 1958, p. 249

[5] A.E. Vol, *Stroeniye i Svoistva Dvoynikh Metallicheskikh System*, Vol 1, Fizmatgiz, Moskwa, 1962, p. 679

[6] T.B. Massalski, J.L. Murray, L.H. Bennett, and H. Baker (Eds.), *Binary Alloy Phase Diagrams*, Vol 1, American Society of Metals, Metals Park, OH, 1986, p. 351

[7] H. Okamoto, B-Fe (Boron-Iron), *J. Phase Equil. Diffusion*, Vol 25, 2004, p. 297-298

[8] V.I. Dybkov, W. Lengauer, and K. Barmak, Formation of Boride Layers at the Fe–10% Cr Alloy-Boron Interface, *J. Alloys Comp.*, Vol 398, 2005, p. 113-122

[9] J. Brandstötter and W. Lengauer, Multiphase Reaction Diffusion in Transition Metal-Boron Systems, *J. Alloys Comp.*, Vol 262-263, 1997, p. 390-396

[10] S. S. Gorelik, L. N. Rastorguev, and Yu. A. Skakov, *Rentgenograficheskiy i Elektronno-Opticheskiy Analiz*, *Prilozheniya*, Metallurgiya, Moskwa, 1970, p. 29

[11] M. Carbucicchio and G. Palombarini, Effects of Alloying Elements on the Growth of Iron Boride Coatings, *J. Mater. Sci. Lett.*, Vol 6, 1987, p. 1147-1149

[12] C. Martini, G. Palombarini, and M. Carbucicchio, Mechanism of Thermochemical Growth of Iron Borides on Iron, *J. Mater. Sci.*, Vol 39, 2004, p. 933-937

[13] K.P. Gurov, B.A. Kartashkin, and YU.E. Ugaste, *Vzaimnaya Diffusiya v Mnogofaznikh Metallicheskikh Sistemakh*, Nauka, Moskwa, 1981

[14] W. Seith, *Diffusion in Metallen*, Springer, Berlin, 1955

[15] K. Hauffe, *Reaktionen in und an festen Stoffen*, Springer, Berlin, 1955

[16] V.I. Arkharov, O Kinetike Reaktsionnoy Diffuzii v Sistemakh s Neskol'kimi Promezhutochnymi Fazami, *Fiz. Metall. Metalloved.*, Vol 8, 1959, p. 193-204

[17] B. Schröder and V. Leute, Solid Sate Reactions and Transport Properties in the Quasi-Binary System AgJ/RbJ, *J. Phys. Chem. Solids*, Vol 41, 1980, p. 827-835

[18] A.T. Fromhold and N. Sato, Quasy-Steady-State Growth of Layered Two-Phase Oxides on Pure Metals, *Oxid. Metals*, Vol 16, 1981, p. 203-220

[19] O.V. Dybkov and V.I. Dybkov, Analytical Treatment of Diffusional Growth Kinetics of Two Intermetallic-Compound Layers, *J. Mater. Sci. Lett.*, Vol 39, 2004, p. 6615-6617

[20] V.I. Dybkov, *Reaction Diffusion and Solid State Chemical Kinetics*, The IPMS Publications, Kyiv, 2002 (free access http://users.i.com.ua/~dybkov/V/)

[21] L. G. Voroshnin, *Borirovaniye Promyshlennikh Staley i Chugunov*, Belarus, Minsk, 1981